COMPARATIVE PHARMACOKINETICS AND BIODISTRIBUTION OF HAEE AND HASS PEPTIDES

Ivanova AV ✉, Lazareva PA, Kuzmichev IA, Vadekhina VV, Kosykh AV, Gurskaya NG, Abakumov MA

Research Institute of Translational Medicine, Pirogov Russian National Research Medical University, Moscow, Russia

Due to the limited availability of advanced methods to diagnose Alzheimer's disease, small molecules and short peptides capable of specifically biniding β-amyloid are of special interest. The study aimed to perform comparative assessment of pharmacokinetics and biodistribution of two model peptides, HAEE (His-Ala-Glu-Glu) and HASS (His-Ala-Ser-Ser), as potential platforms for the development of diagnostic kits, as well as to determine the relationship between the peptide structure and organotropism. The study involving BALB/c mice (*n* = 10) was conducted using the fluorescence labeled compounds. We used *in vivo* IVIS imaging, *ex vivo* fluorescence microscopy, and pharmacokinetic analysis. The results showed fundamental differences: the negatively charged HAEE was accumulated mainly in the kidney ($T_{½}β$ = 4.39 h) due to tubular reabsorption, while neutral HASS was soon captured by the liver ($T_{½}β$ = 2.76 h). The data obtained demonstrate the key role of amino acid composition in determining organotropism and open prospects for the development of organ-specific peptide systems.

Keywords: HAEE peptide, HASS peptide, BALB/c healthy mice, HAEE pharmacokinetics, HASS pharmacokinetics, *in vivo* fluorescence imaging (IVIS), blood brain barrier, HAEE biodistribution, HASS biodistribution

Funding: the study was conducted under the State Assignment "Development of a Radiopharmaceutical for the Diagnosis of Alzheimer's disease Using the HAEE Tetrapeptide as a Vector Molecule", EGISU R&D registration number 1024110600012-8-3.2.25;3.2.26;3.2.12.

Author contribution: Ivanova AV — literature review, BALB/c mouse model experimental research, ensuring transcardiac perfusion of all organs, manuscript writing; Lazareva PA — BALB/c mouse model experimental research, ensuring transcardiac perfusion of all organs, analysis of the results, manuscript writing; Kuzmichev IA — synthesis of HAEEGGGGK-Cy5 and HASSGGGGGK-Cy5 fluorescent peptides; Vadekhina VV — intravenous tail vein injection of HAEEGGGGK-Cy5 and HASSGGGGGK-Cy5 peptides, ensuring transcardiac perfusion of all organs; Kosykh AV — fixation, histology slide preparation for microscopic imaging, imaging and manuscript writing; Gurskaya NG — imaging using the fluorescence microscope and analysis, manuscript writing; Abakumov MA — goal setting, developing the study design, manuscript writing; all the authors contributed to preparation of the paper equally, they confirmed compliance of their authorship with the international ICMJE criteria.

Compliance with ethical standards: the study approved by the Ethics Committee of the Pirogov Russian National Research Medical University (protocol 03/2025 dated 23 January 2025) was conducted in accordance with the principles of Good Laboratory Practice (Order of the Ministry of Health of the Russian Federation No. 708n dated 23.08.2010, Directive 2010/63/EU of the European Parliament and of the Council on the protection of animals used for scientific purposes).

✉ **Correspondence should be addressed:** Anna V. Ivanova
Ostrovityanova, 1, stroenie 1, Moscow, 117513, Russia; super.fosforit@yandex.ru

Received: 10.07.2025 **Accepted:** 24.07.2025 **Published online:** 31.07.2025

DOI: 10.24075/brsmu.2025.036

СРАВНИТЕЛЬНАЯ ФАРМАКОКИНЕТИКА И БИОРАСПРЕДЕЛЕНИЕ ПЕПТИДОВ HAEE И HASS

А. В. Иванова ✉, П. А. Лазарева, И. А. Кузьмичев, В. В. Вадехина, А. В. Косых, Н. Г. Гурская, М. А. Абакумов

Научно-исследовательский институт трансляционной медицины, Российский национальный исследовательский медицинский университет имени Н. И. Пирогова, Москва, Россия

В связи с ограниченной доступностью современных методов диагностики болезни Альцгеймера особый интерес представляют малые молекулы и короткие пептиды, способные специфично связываться с β-амилоидом. Целью работы было провести сравнительное изучение фармакокинетики и биораспределения двух модельных пептидов — HAEE (His-Ala-Glu-Glu) и HASS (His-Ala-Ser-Ser) как потенциальных платформ для разработки диагностических систем и установить взаимосвязь между структурой пептидов и их органотропностью. Исследование выполнено на мышах линии BALB/c (*n* = 10) с использованием флуоресцентно меченых соединений. Применяли IVIS-визуализацию *in vivo*, флуоресцентную микроскопию *ex vivo* и фармакокинетический анализ. Результаты выявили принципиальные различия: HAEE с отрицательным зарядом преимущественно накапливался в почках ($T_{½}β$ = 4,39 ч) благодаря реабсорбции в канальцах, тогда как нейтральный HASS быстро захватывался печенью ($T_{½}β$ = 2,76 ч). Полученные данные демонстрируют ключевую роль аминокислотного состава в определении органотропности и открывают перспективы для разработки органоспецифичных пептидных систем.

Ключевые слова: пептид HAEE, пептид HASS, BALB/c здоровые мыши, фармакокинетика HAEE, фармакокинетика HASS, *in vivo* флуоресцентная визуализация (IVIS), гематоэнцефалический барьер, биораспределение HAEE, биораспределение HASS

Финансирование: работы выполнены в рамках Государственного задания «Создание радиофармацевтического лекарственного препарата для диагностики болезни Альцгеймера с использованием тетрапептида HAEE в качестве векторной молекулы», регистрационный номер ЕГИСУ НИОКТР 1024110600012-8-3.2.25;3.2.26;3.2.12.

Вклад авторов: А. В. Иванова — обзор литературы, экспериментальные исследования на мышиной модели BALB/c, проведение транскардиальной перфузии всех органов, подготовка рукописи; П. А. Лазарева — экспериментальные исследования на модели мышей BALB/c, проведение транскардиальной перфузии всех органов, анализ полученных результатов, подготовка рукописи; И. А. Кузьмичев — синтез флуоресцентного пептида HAEEGGGGK-Cy5 и HASSGGGGGK-Cy5; В. В. Вадехина — внутривенное введение пептида HAEEGGGGK-Cy5 и HASSGGGGGK-Cy5 через хвостовую вену, проведение транскардиальной перфузии всех органов; А. В. Косых — фиксация, подготовка гистологических срезов для съемки на микроскопе, съемка и подготовка рукописи; Н. Г. Гурская — получение изображений на флуоресцентном микроскопе и анализ, подготовка рукописи; М. А. Абакумов — постановка цели, разработка дизайна исследования, подготовка рукописи; все авторы внесли равнозначный вклад в подготовку публикации, подтверждают соответствие своего авторства международным критериям ICMJE.

Соблюдение этических стандартов: исследование одобрено этическим комитетом РНИМУ им Н. И. Пирогова Минздрава России (номер протокола 03/2025 от 23 января 2025 г.), проведено в соответствии с принципами надлежащей лабораторной практики (Приказ Министерства здравоохранения Российской Федерации № 708н от 23.08.2010, Директива 2010/63/EU Европейского парламента и Совета о защите животных, используемых в научных целях).

✉ **Для корреспонденции:** Анна Валерьевна Иванова
ул. Островитянова, д. 1, стр. 1, г. Москва, 117513, Россия; super.fosforit@yandex.ru

Статья получена: 10.07.2025 **Статья принята к печати:** 24.07.2025 **Опубликована онлайн:** 31.07.2025

DOI: 10.24075/vrgmu.2025.036

Alzheimer's disease remains one of the most socially significant neurodegenerative disorders and the main cause of dementia in elderly people [1, 2]. The disease prevalence grows exponentially with age: 53 new cases per 1000 people aged 65–74; 170 new cases per 1000 people aged 75–84, and 230 new cases per 1000 people aged over 85 [3, 4]. The disease pathogenesis is complex and multifaceted. However, this process is rather often accompanied by accumulation of β-amyloid (Aβ) in the form of senile plaques in the cerebral cortex [5]. Aβ represents a peptide with the length of 39–43 amino acid bases that is generated from the Aβ precursor protein (APP) [6]. This unique APP breakdown process provides important targets for treatment of Alzheimer's disease [7]. Two major peptides have the length of 40 ($Aβ_{40}$) and 42 ($Aβ_{42}$) amino acid bases. $Aβ_{42}$ is prone to aggregation *in vivo*, it is often considered to be more toxic [8, 9]. $Aβ_{42}$ accumulation triggers the cascade of abnormalities including formation of oligomers and fibrils, neuroinflammation activation, synaptic transmission impairment, neuronal death [6, 10, 11]. Unfortunately, the in-depth study of the amyloid hypothesis and other pathogenetic hypotheses has failed to produce any truly effective therapeutic strategy, while such strategies have been developed since the disease was first described in 1906 [12]. Modern methods to diagnose Alzheimer's disease are still inaccessible for widespread use due to technical complexity and significant expenses. In this regard, small molecules capable of specific binding to Aβ are of special interest; their versatility and the possibility of chemical modification open up prospects for the development of more affordable diagnostic platforms. Among such molecules, short peptide sequences, particularly tetrapeptides HAEE (His-Ala-Glu-Glu) and HASS (His-Ala-Ser-Ser) that combine high affinity for β-amyloid, inhibition of its aggregation, good pharmacokinetic properties, and the ability to cross the blood-brain barrier, turned out to be the most promising [13]. To ensure realization of their diagnostic potential, it is necessary to thoroughly assess pharmacokinetic properties, including biodistribution, the ability to cross the blood-brain barrier, and the dynamics of elimination from the body. This study is focused on comprehensive characterization of these parameters involving the use of the fluorescence labeled HAEE and HASS analogues in animal models.

The study aimed to determine pharmacokinetic parameters of the HAEE and HASS tetrapeptides in healthy animals, including half-life ($T_{1/2}$), in order to assess the tetrapeptide biodistribution, stability *in vivo*, and prospects for further use as a basis for radiopharmaceuticals or therapeutic agents.

METHODS

All the experiments were conducted at the research laboratory of the Deparment of Medical Nanobiotechnology, as well as at the Department of Regenerative Medicine of the Research Institute of Translational Medicine, Pirogov Russian National Research Medical University.

IVIS imaging *in vivo*/*ex vivo*

Female BALB/c mice aged 3 months with the weight of 20–25 g were purchased brom the breeding nursery of the Center of Biomedical Technology of the Federal Medical Biological Agency of Russia, Stolbovaya branch (Moscow region, Russia).

Mice had ad libitum access to food and water. The animals received extruded complete feed for laboratory animals: mice, rats, hamsters (Laborantsnab, Russia). Daytime was 12 h (between 7:00 and 19:00); illuminance during the light part of the cycle was 70–90 lx; the temperature in the room where the animals were permanently kept was 22 °C.

Each experiment involved five animals. The test peptides were HAEEGGGGK-Cy5 and HASSGGGGK-Cy5 (purity > 95% based on the HPLC data). The peptides were dissolved in the sterile 0.9 % NaCl solution to the final concentration of 250 μM before administration. The resulting solutions were filtered through the 0.22 μm filter and injected intravenously in the tail vein (n = 4 animals per group) in the amount of 100 μL. The control group was administered 100 μL of the 0.9% NaCl solution.

Intravital fluorescence imaging was performed using the IVIS Spectrum CT imaging system (Perkin Elmer, USA) at the time points of 15 min, 1 h, 2 h, 3 h, 4 h, 5 h, 6 h, 24 h after administration. Fluorescence imaging was accomplished under inhalation anesthesia with 2% isoflurane (Aerrane, Baxter HealthCareCorporation, USA) mixed with air.

The animals were ansthesized by intraperitoneal injection of tiletamine (Zoletil, Virbac, France) for further experiments. Then transcardial perfusion was performed. For that the right atrium was incised, the cannula was inserted in the left ventricle, and blood channels were washed sequentially with the sterile phosphate buffered saline (Sigma-Aldrich, USA) and HistoSafe 10% buffered formalin (Biovitrum, Russia). The organs were retrieved, and *ex vivo* fluorescence imaging was performed.

Fluorescence analysis and kinetic modeling

Photon emission was calculated using the Living Image 4.3 software with selection of the region of interest (ROI). Fluorescence values of the control animal for each time point were subtracted from the animals' fluorescence values in order to eliminate systematic measurement errors. The same was done for the organs.

Widefield fluorescence microscopy

The 10 μm cryosections were cut using the HM525 cryo microtome (Thermo Scientific, USA). For further analysis,

Table 1. Dynamic changes in the mean fluorescence intensity (p/sec/cm^2/sr) injection of the HAEE and HASS fluorescence peptides

Time, h	HAEE (Mean ± SD)*	HASS (Mean ± SD)*
0.25	$(1.23 \pm 0.18) \times 10^9$	$(1.31 \pm 0.19) \times 10^9$
1	$(4.61 \pm 0.51) \times 10^8$	$(2.11 \pm 0.18) \times 10^8$
2	$(1.76 \pm 0.16) \times 10^8$	$(8.69 \pm 0.75) \times 10^7$
3	$(1.21 \pm 0.09) \times 10^8$	$(6.04 \pm 1.01) \times 10^7$
4	$(9.53 \pm 1.07) \times 10^7$	$(5.57 \pm 0.92) \times 10^7$
5	$(7.53 \pm 0.82) \times 10^7$	$(4.93 \pm 0.94) \times 10^7$
6	$(7.87 \pm 0.99) \times 10^7$	$(4.20 \pm 0.71) \times 10^7$
24	$(3.14 \pm 0.28) \times 10^7$	$(1.97 \pm 0.23) \times 10^7$

Note: * — the data are presented as the mean ± standard deviation (Mean ± SD) for n = 4

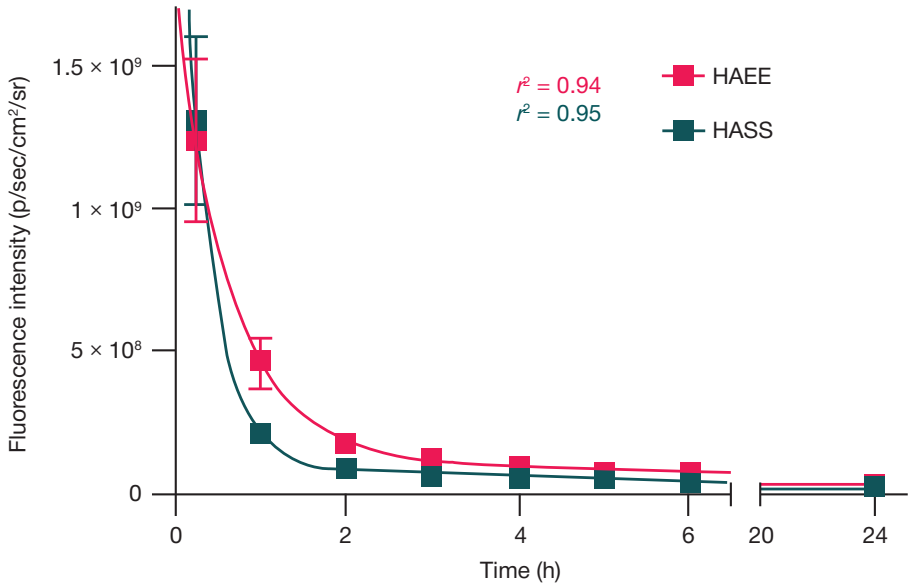

Fig. 1. *In vivo* fluorescence kinetic curves of the studied HAEE (r^2 = 0.94) and HASS (r^2 = 0.95) peptides

sections were fixed in the 10% buffered formalin (Biovitrum, Russia) for 15 min, sequentially triple washed with phosphate buffered saline containing no Ca^{2+} and Mg^{2+} (PanEco, Russia), and embedded in the VECTASHIELD Atifade Mounting Medium with DAPI (VectorLabs, USA). Images were acquired using the EVOS FL Auto imaging system (Thermo Scientific, USA).

Statistical analysis

Data analysis was performed in GraphPad Prism 8.0.1 (GraphPad Software, USA). The graph of the fluorescence signal intensity as a function of time was presented as mean values with standard deviations and the trend line for the two-chamber model. The graph of ex vivo drug accumulation in the organs contained the mean value, maximum and minimum values for the group.

RESULTS

Teporary changes in fluorescence intensity were reported after a single intravenous injection of the HAEE and HASS fluorescence peptides to BALB/c mice (Table 1). Both compounds showed rapid systemic absorption reaching the maximum concentration 0.25 h after administration. Furthemore, HASS ((1.31 ± 0.19) × 10^9 p/sec/cm²/sr) showed the 6.5% higher fluorescence intensity compared to HAEE ((1.23 ± 0.18) × 10^9 p/sec/cm²/sr) with subsequent exponential decrease in indicators. The findings are more clearly demonstrated in Fig. 1.

Plotting of the resulting kinetic profiles on a logarithmic scale suggests the two-chamber model of the HASS and HAEE peptide elimination (Fig. 2).

The HAEE and HASS kinetic curves (Fig. 1, 2) described by the two-chamber model ($Ap = A_1 \cdot e^{-\alpha t} + A_2 \cdot e^{-\beta t}$) demonstrate

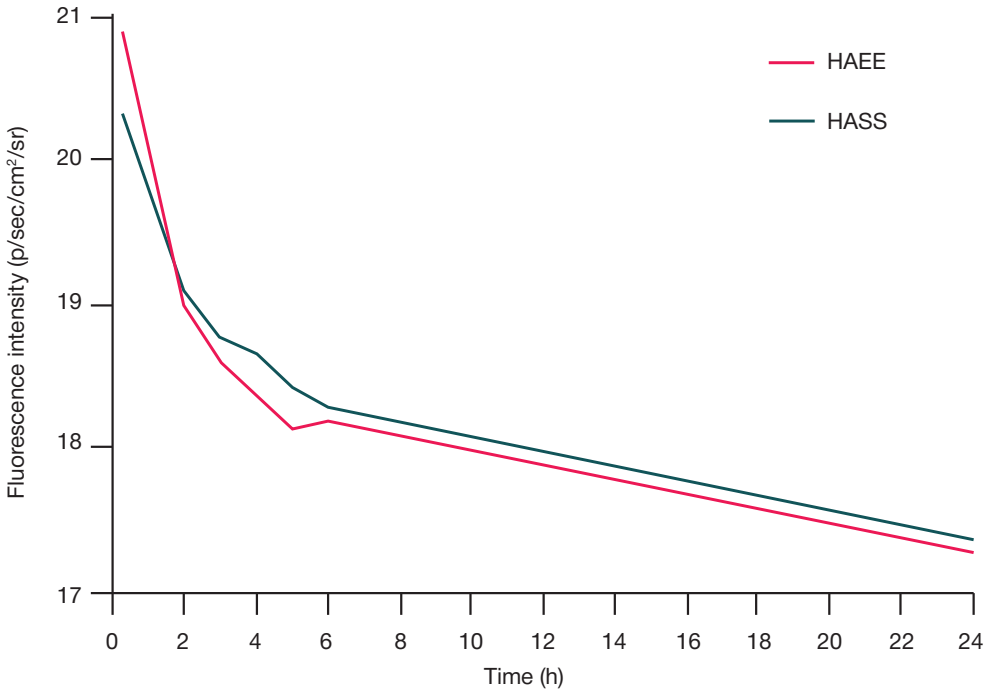

Fip. 2. Comparative kinetics of the HAEE and HASS peptide elimination

Table 2. Comparison of the HAEE and HASS pharmacokinetic parameters after intravenous administration

Parameter	HAEE	HASS
Rapid elimination phase, %	93.37	96.43
α, h	1.6	3.11
β, h	0.16	0.25
$T_{1/2}$ of the rapid distribution phase, h	0.43	0.22
$E_{1/2}$ of the elimination phase, h	4.39	2.76
A_1 of the rapid distribution phase, p/sec/cm²/sr	1.64×10^9	2.61×10^9
A_2 of the elimination phase, p/sec/cm²/sr	1.16×10^8	9.67×10^7
AUC (0→∞), h * p/sec/cm²/sr	3.69×10^9	1.51×10^9

considerable differences in elimination parameters (Table 2): HASS is characterized by the dominance of the rapid phase (96.43% vs. 93.37%), higher rate constant α (3.11 h^{-1} vs. 1.6 h^{-1}) and shorter $T_{½}α$ (0.22 h vs. 0.43 h), which is correlated to the steep initial decline on the graphs, while HAEE showing prolonged elimination with the extended $T_{½}β$ (4.39 h vs. 2.76 h) is characterized by the gentle slope on the kinetic curve and the large AUC (3.69×10^9 vs. 1.51×10^9 h· p/sec/cm²/sr), which suggests its potential advantage for the long diagnosis.

Ex vivo assessment of the HAEE and HASS peptide accumulation was performed 24 h after injection. According to the data obtained (Fig. 3), the peptides show different organ specificity: HAEE is localized mainly in the kidney, while HASS is localized mainly in the liver. Both compounds are accumulated in the lung and brain showing no significant intergroup differences ($p > 0.05$). As for the heart and spleen, fluorescence intensity in the HAEE group was significantly higher, than in the HASS group ($p < 0.05$).

The HAEE longer half-life results from the fact that it is eliminated mainly by the kidney, which has been confirmed by fluorescence microscopy of the sections that has revealed intense fluorescence signal accumulation in the renal tubular epithelium (Fig. 4), which is consistent with the IVIS data (Fig. 5), where the kidneys show stronger fluorescence signal compared to other organs within 24 h, while HASS is accumulated primarily in the liver (Fig. 5).

Assessment of representative microphotos of the mouse kidney tissue sections confirms increased HAEE content in the form of accumulation of the large number of Cy^{5+} aggregates in the cells of renal proximal tubules (Fig. 4A, B) compared to HASS (Fig. 4C, D).

DISCUSSION

Our studies have revealed considerable differences in biodistribution of the HAEE and HASS peptides, which can be explained by their structural and functional features. HAEE having low molecular weight (< 2 kDa) and weak negative charge demonstrates primarily renal excretion. Such process is typical for low molecular weight peptides [14], which are reabsorbed through pinocytosis after glomerular filtration. The presence of the Cyanine 5 (Cy5) fluorescent label in the peptide structure can increase its lipophilicity, contributing to penetration through the cell membranes, specifically in the epithelium of the renal proximal tubules, which explains the reported compound accumulation in the kidney tissue. Nor can the possibility be excluded that the peptide specifically interacts with the cellular receptors. However, this aspect requires further research. HAEE can enter the liver by passive transport through the membranes of hepatocytes and Kupffer cells. Furthermore, considering the key role of liver in metabolism and detoxification, accumulation of the peptide in this organ can be associated with its biotransformation or active transport via hepatocytes. Upon systemic administration, pulmonary epithelium is also permeable for small lipophilic molecules [15], which is confirmed by detection of fluorescence signal in the lung. Experimental studies involving BALB/c mice have shown

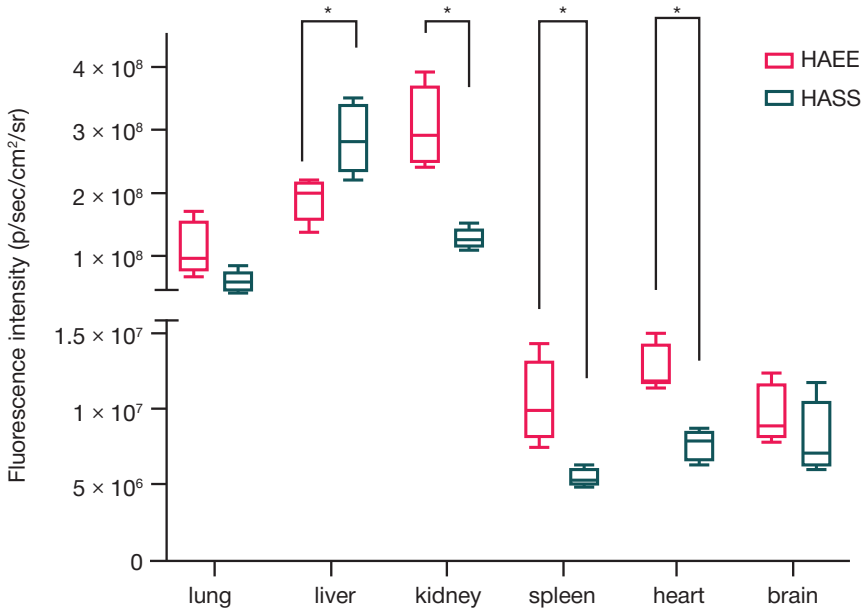

Fig. 3. *Ex vivo* assessment of the HAEE and HASS accumulation in the organs 24 h after intravenous administration. * — $p < 0.05$, significance of intergroup differences based on the Mann–Whitney U-test

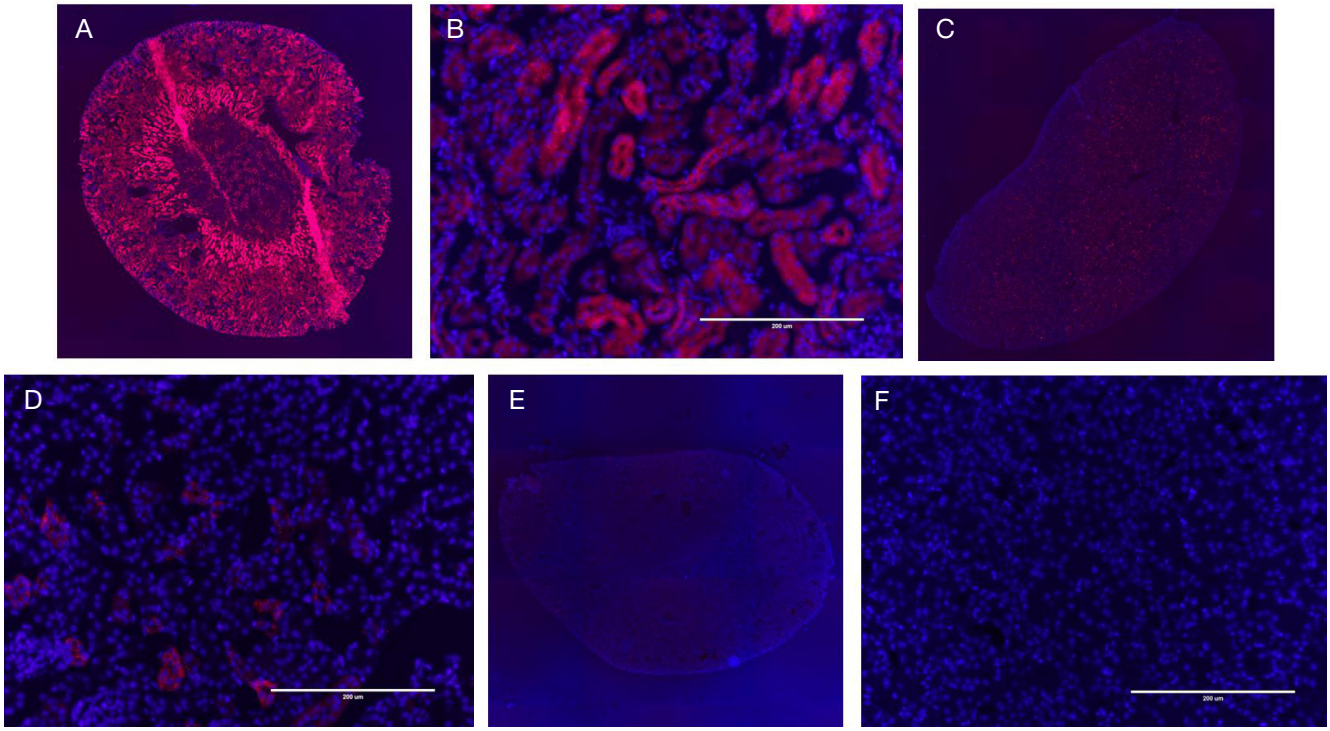

Fig. 4. Histological analysis of the mouse kidney tissue after the HAEE and HASS systemic administration. **A**, **B**. Localization of the Cy5-labeled HAEE (*red*) in the mouse kidney 24 h after intravenous administration. **A**. Giant section of the mouse kidney. **B**. Accumulation of fluorescent granules in epithelial cells of the renal proximal tubules. **C**, **D**. Localization of the Cy5-labeled HASS (*red*) in the mouse kidney 24 h after intravenous administration. **C**. Giant section of the mouse kidney. **D**. Accumulation of fluorescent granules in epithelial cells of the renal proximal tubules. **E**, **F**. Kidney of the control mice 24 h after intravenous administration of saline. **E**. Giant section of the kidney. **F**. Magnified image of the kidney tissue obtained by superimposing red and blue fluorescence. The nuclei are DAPI stained (*blue*). Scale bar 200 μm

that HAEE is characterized primarily by renal excretion, which is confirmed by three key observations: 1) high fluorescence intensity in the kidney 24 h after administration recorded by both IVIS imaging and fluorescence microscopy; 2) prolonged half-life ($T_{½}\beta$ = 4.39 h), which is explained by reabsorption in the renal tubules; 3) rapid initial elimination ($T_{½}\alpha$ = 0.43 h) suggesting that there are no stable complexes with blood plasma proteins.

In contrast to HAEE, the neutrally charged HASS peptide demonstrates fundamentally different pharmacokinetic characteristics. Its peak fluorescence signal is 6.5% higher than that of HAEE, which is likely to be due to reduced binding to the tissue structures. HASS is characterized by enhanced elimination with the half-life of $T_{½}\alpha$ = 0.22 h and $T_{½}\beta$ = 2.76 h resulting probably from active capture by hepatocytes. The ex vivo testing 24 h after administration confirmed selective accumulation of the peptide in the liver tissue.

Despite similar size (< 2 kDa), HAEE shows the 1.7 times better blood-brain barrier permeability (AUC (0→∞)), which is likely to be due to electrostatic effects and the features of interaction with transport systems.

The findings demonstrate considerable differences in the distribution of the studied peptides across organs. In particular, it has been found that HAEE is excreted primarily by the kidney, which determines its potential diagnostic value for renal disorders. In contrast to HAEE, HASS shows high hepatospecificity and high hepatic metabolism rate, which allows one to consider it as a promising basis for the development of the delivery systems targeting the liver. The presence of the Cy5 label increases lipophilicity of both peptides, which contributes to their transport through the cell membranes. However, the limited crossing of the blood-brain barrier (especially that of HASS) suggests the need for structural optimization for the use in neurodiagnosis. Further research is required for better understanding of the mechanisms underlying biodistribution of tetrapeptides: 1) identification of the transport systems (megalin/OATP (organic anion transporting polypeptide)); 2) complete metabolic profile in biological fluids; 3) correlation between structural alterations of peptides and their distribution across the organs.

CONCLUSIONS

Thus, the comparative study conducted has revealed fundamental differences in the HAEE and HASS behavior

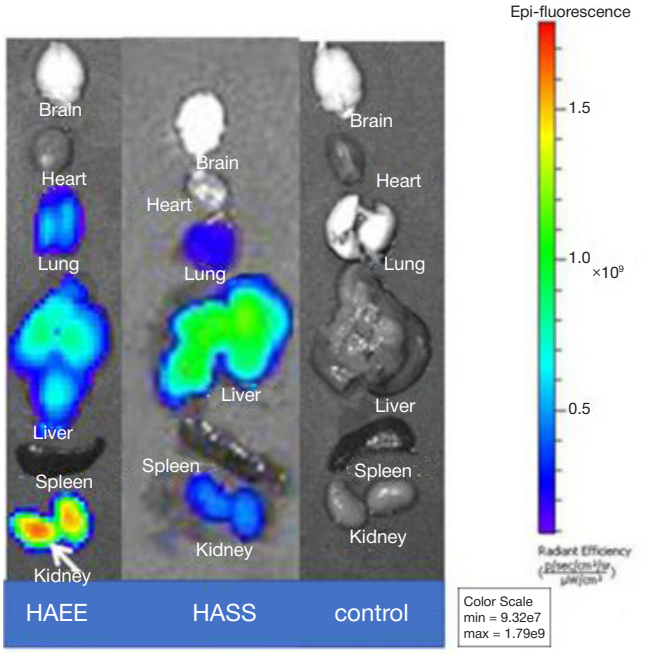

Fig. 5. HAEE and HASS organ specificity within 24 h (IVIS). *White arrow* points to the kidneys with maximum buildup. Color scale: from blue (min) to red (max)

in vivo. The peptides demonstrate no only different organ tropism, but also fundamentally different pharmacokinetic profiles (including half-life, $T_{1/2}$), which opens up the prospects for differentiated use of those in the diagnosis and targeted drug delivery. It has been found that HAEE with short $T_{1/2}$ and renal excretion is promising for the development of diagnostic radiopharmaceuticals, while HASS showing hepatotropism and rapid hepatic metabolism is of intrest in terms of developing the targeted delivery systems. It should be noted that the results were obtained using the healthy mouse model. These data that should be further tested in model transgenic animals with Alzheimer's disease now suggest new strategies for complex therapy combining the organ-specific peptide transport and pathogenetic effects. Furthermore, the impact of fluorescent label on pharmacokinetic parameters should be assessed separately.

References

1. Huang LK, Kuo HY, Chen HJ, et al. Clinical trials of new drugs for Alzheimer disease: a 2020–2023 update. J Dent Res. 2023; 88 (3): 1–19.
2. Facts D. Alzheimer's disease facts and figures report: executive summary. Alzheimers Dement. 2024; 20 (5): 40–42.
3. Adlard PA, Bush AI. A review of β-amyloid neuroimaging in Alzheimer's disease. Front Neurosci. 2014; 8 (OCT): 1–23.
4. Thies W, Bleiler L. 2011 Alzheimer's disease facts and figures. Alzheimers Dement. 2011; 7 (2): 208–44.
5. Tackenberg C, Kulic L, Nitsch RM. Familial Alzheimer's disease mutations at position 22 of the amyloid β-peptide sequence differentially affect synaptic loss, tau phosphorylation and neuronal cell death in an ex vivo system. PLoS One. 2020; 15 (9): 1–14.
6. Hayne DJ, Lim S, Donnelly PS. Metal complexes designed to bind to amyloid-β for the diagnosis and treatment of Alzheimer's disease. Chem Soc Rev. 2014; 43 (19): 6701–15.
7. Carroll CM, Li YM. Physiological and pathological roles of the γ-secretase complex. Brain Res Bull. 2016; 126: 199–206.
8. Haass C, Selkoe DJ. Soluble protein oligomers in neurodegeneration: lessons from the Alzheimer's amyloid β-peptide. Nat Rev Mol Cell Biol. 2007; 8 (2): 101–12.
9. Citron M. Alzheimer's disease: strategies for disease modification. Nat Rev Drug Discov. 2010; 9 (5): 387–98.
10. Masters CL, Simms G, Weinman NA, et al. Molecular mechanisms for Alzheimer's disease: implications for neuroimaging and therapeutics. J Neurochem. 2006; 97 (6): 1700–25.
11. Masters CL, Beyreuther K. Science, medicine, and the future: Alzheimer's disease. BMJ. 1998; 316 (7129): 446.
12. Hippius H, Neundörfer G. The discovery of Alzheimer's disease. Dialogues Clin Neurosci. 2003; 5 (1): 101–8.
13. Zolotarev YA, Dadayan AK, Bocharov EV, et al. Pharmacokinetics and molecular modeling indicate nAChRα4-derived peptide HAEE goes through the blood-brain barrier. Biomolecules. 2021; 11 (6): 902.
14. Maack T, Johnson V, Kau ST, et al. Renal filtration, transport, and metabolism of low-molecular-weight proteins: a review. Kidney Int. 1979; 16 (3): 251–70.
15. Agu RU, Ugwoke MI, Armand M, et al. The lung as a route for systemic delivery of therapeutic proteins and peptides. Respir Res. 2001; 2 (4): 198–209.

Литература

1. Huang LK, Kuo HY, Chen HJ, et al. Clinical trials of new drugs for Alzheimer disease: a 2020–2023 update. J Dent Res. 2023; 88 (3): 1–19.
2. Facts D. Alzheimer's disease facts and figures report: executive summary. Alzheimers Dement. 2024; 20 (5): 40–42.
3. Adlard PA, Bush AI. A review of β-amyloid neuroimaging in Alzheimer's disease. Front Neurosci. 2014; 8 (OCT): 1–23.
4. Thies W, Bleiler L. 2011 Alzheimer's disease facts and figures. Alzheimers Dement. 2011; 7 (2): 208–44.
5. Tackenberg C, Kulic L, Nitsch RM. Familial Alzheimer's disease mutations at position 22 of the amyloid β-peptide sequence differentially affect synaptic loss, tau phosphorylation and neuronal cell death in an ex vivo system. PLoS One. 2020; 15 (9): 1–14.
6. Hayne DJ, Lim S, Donnelly PS. Metal complexes designed to bind to amyloid-β for the diagnosis and treatment of Alzheimer's disease. Chem Soc Rev. 2014; 43 (19): 6701–15.
7. Carroll CM, Li YM. Physiological and pathological roles of the γ-secretase complex. Brain Res Bull. 2016; 126: 199–206.
8. Haass C, Selkoe DJ. Soluble protein oligomers in neurodegeneration: lessons from the Alzheimer's amyloid β-peptide. Nat Rev Mol Cell Biol. 2007; 8 (2): 101–12.
9. Citron M. Alzheimer's disease: strategies for disease modification. Nat Rev Drug Discov. 2010; 9 (5): 387–98.
10. Masters CL, Simms G, Weinman NA, et al. Molecular mechanisms for Alzheimer's disease: implications for neuroimaging and therapeutics. J Neurochem. 2006; 97 (6): 1700–25.
11. Masters CL, Beyreuther K. Science, medicine, and the future: Alzheimer's disease. BMJ. 1998; 316 (7129): 446.
12. Hippius H, Neundörfer G. The discovery of Alzheimer's disease. Dialogues Clin Neurosci. 2003; 5 (1): 101–8.
13. Zolotarev YA, Dadayan AK, Bocharov EV, et al. Pharmacokinetics and molecular modeling indicate nAChRα4-derived peptide HAEE goes through the blood-brain barrier. Biomolecules. 2021; 11 (6): 902.
14. Maack T, Johnson V, Kau ST, et al. Renal filtration, transport, and metabolism of low-molecular-weight proteins: a review. Kidney Int. 1979; 16 (3): 251–70.
15. Agu RU, Ugwoke MI, Armand M, et al. The lung as a route for systemic delivery of therapeutic proteins and peptides. Respir Res. 2001; 2 (4): 198–209.